## Efficient Hybrid Symbolic-Numeric Computational Method for Piecewise Linear Systems with Coulomb Friction

#### Amir Shahhosseini

Department of Mechanical and Aerospace Engineering The Ohio State University Columbus, OH, USA 43235 Email: shahhosseini.3@osu.edu

## Meng-Hsuan Tien

Department of Power Mechanical Engineering National Tsing Hua University Hsinchu, Taiwan 30013 Email: mhtien@pme.nthu.edu.tw

#### Kiran D'Souza \*

Department of Mechanical and Aerospace Engineering The Ohio State University Columbus, OH, USA 43235 Email: dsouza.60@osu.edu

A wide range of mechanical systems have gaps, cracks, intermittent contact or other geometrical discontinuities while simultaneously experiencing Coulomb friction. A piecewise linear model with discontinuous force elements is discussed in this paper that has the capability to accurately emulate the behavior of such mechanical assemblies. The mathematical formulation of the model is standardized via a universal differential inclusion and its behavior, in different scenarios, is studied. In addition to the compatibility of the proposed model with numerous industrial systems, the model also bears significant scientific value since it can demonstrate a wide spectrum of motions, ranging from periodic to chaotic. Furthermore, it is demonstrated that this class of models can generate a rare type of motion, called weakly chaotic motion.

After their detailed introduction and analysis, an efficient hybrid symbolic-numeric computational method is introduced that can accurately obtain the arbitrary response of this class of nonlinear models. The proposed method is capable of treating high dimensional systems and its proposition omits the need for utilizing model reduction techniques for a wide range of problems. In contrast to the existing literature focused on improving the computational performance when analyzing these systems when there is a periodic response, this method is able to capture transient and non-stationary dynamics and is not restricted to only steady state periodic responses.

#### 1 Introduction

The existence of gaps, pre-stress, intermittent contact, cracks, and other geometrical discontinuities has the capability to fundamentally alter the dynamical behavior of mechanical assemblies [1–3]. Consequently, accurate modelling of these discontinuities plays a crucial role in correct estimation of their behavior and facilitates the capturing of the entirety of the assembly's dynamics. To propose adequate mathematical models that accurately represent natural systems or engineered structures, discontinuous models are often required. Mathematical models with piecewise linear (PWL) nonlinearities are known to be an excellent choice and form a significant class of such models [4–7].

Nonetheless, despite the enhanced accuracy of PWL models, they often fail to precisely emulate the behavior of the mechanical assemblies that they intend to model. There are a number of reasons for this incompatibility, but the main reason for the shortcoming of these PWL models is concealed in the omittance of dry friction [8]. The relative motion of mechanical components unavoidably gives rise to the emergence of Coulomb friction [9–11]. An alternative reason for this incompatibility lies in the modelling of the contacting material. The study by Saito et al. [12] examines the vibration of PWL systems and demonstrates a difference between the data obtained from the simulation of PWL models and experimental data. The experimental setup of the aforementioned study covers the masses with relatively thick viscoelastic sheets but the dynamic model of these sheets are not accounted for in the PWL model. These viscoelastic sheets are known to demonstrate fractional order behavior [13] and

<sup>\*</sup>Address all correspondence related to ASME style format and figures to this author.

the study by Homaeinezhad and Shahhosseini [14] reports that the omittance of the fractional elements can severely alter the dynamical behavior.

To obtain a complete model for the discontinuous systems of interest, the corresponding PWL models must include a complete set of discontinuities including the one induced by Coulomb friction. This new model is piecewise linear with discontinuous force elements (PWLDFE) where the discontinuous force elements are intended to model the multi-valued forces. In addition to the application of PWLDFE models in mechanical, civil and aerospace engineering's real world problems [15, 16], these models also possess significant scientific importance [17]. Such mathematical models are capable of illustrating a wide spectrum of motion, ranging from periodic to fully chaotic [18, 19]. It is noteworthy to mention that the PWLDFE models can also demonstrate a rare type of motion called (slowly) weakly chaotic motion, which is very infrequently encountered in the world of engineering and will be further discussed later in this paper.

Owing to the widespread application of PWLDFE models, it is essential to utilize methods that can evaluate their response efficiently and accurately. The inherent nonlinearity of this class of models precludes the utilization of conventional linear techniques and consequently, nonlinear techniques are required [20]. The existing methods of the literature were initially focused on estimating the steady-state response of nonlinear systems and were limited in terms of applicability. The proposition of the harmonic balance method can be considered as a cornerstone of this class of methodologies [21]. Numerous subsequent studies have been conducted on this foundation that attempted to modify this method to make it further compatible with different nonlinear systems, such as PWL systems [22, 23]. Alternative techniques have since been introduced that employed different approaches [7]. The study by Saito [24] proposed a novel technique that relied on an alternating time and frequency domain analysis to obtain the steady-state characteristics of PWL systems. The studies by Tien and D'Souza [25-28] have also introduced novel methodologies that exploit the limited linearity of PWL systems to obtain the steady-state response of systems with either intermittent contact or Coulomb friction. These methods employ a fusion of numerical and analytical methods to accurately construct the steady-state response and are proven to be very effective for high dimensional systems. In spite of all the advancements in the literature, the problem of analyzing the steady-state behavior of general PWLDFE systems with complex responses remained open. In addition to the deficiency of this class of methods in treating general PWL systems with complex steady-state responses, they also fail to provide insight on the transient and non-stationary response of PWL systems.

To get further acquainted with this class of nonlinear systems, it is beneficial to delve into the mathematical foundations of PWLDFE systems. PWLDFE systems are in fact differential equations with multi-valued mappings on the right-hand side where these mappings usually attempt to represent the effects of geometrical or inherent disconti-

nuities (e.g. intermittent contacts). This class of problems is in fact a generalization of differential equations and is known as differential inclusions and the corresponding systems are known as Filippov systems. They are extensively explored in study Filippov [29] and it is known that no analytical solution exists for the general case in such problems. It is noteworthy to mention that even simple problems of differential inclusions might not have an analytical solution. Consequently, numerical integration (NI) methods are typically employed to obtain the transient or steady-state responses. Conventional NI methods, such as Runge-Kutta or Adams-Bashforth [30, 31] are usually used in this context and have proven effective for the case of simple PWL systems. Nonetheless, with increased complexity, the NI methods are known to require a very small step size [32] and this will inevitably result in large computational costs. Additionally, due to numerical errors, NI methods may not capture the correct response of PWL systems especially when it comes to stick-slip cases [33]. Tien and D'Souza [18] discuss another drawback of NI methods which occurs when the PWL system begins to illustrate signs of chaos. In that case, the numerical errors of NI methods cause a systematic failure in obtaining the accurate response of the PWL systems and the acquired response will quickly diverge from the true response [34, 35].

To overcome the aforementioned shortcomings of the existing methods, a novel method was proposed by Tien and D'Souza [36] with the capability of obtaining the arbitrary response of PWL systems. The introduced method was a combination of numerical methods with analytical techniques that permitted efficient and accurate obtainment of the total response of PWL systems. Their studies [18, 36] demonstrate the computational efficiency of this method and illustrate its superior performance for high dimensional systems. However, their work is only valid for a particular class of PWL systems and fails to treat general PWLDFE systems.

The present work introduces a novel method that can capture the entirety of PWLDFE systems' dynamics, regardless of their complexity. In addition to the aforementioned capabilities, the new method is faster and more accurate than current techniques. It is a hybrid symbolic-numeric computational (HSNC) method that mathematically manipulates the PWLDFE models to cast them into a temporary linear formulation and then exploits this temporary linearity to employ fast linear techniques. A numerical scheme is then used to compute the nonlinear response of PWLDFE models by combining the linear techniques and a switch detection method. This hybrid method provides an efficient and reliable tool for analyzing these systems.

Since numerical integration remains as the only alternative universally implementable method, it is crucial to elucidate the fundamental difference of HSNC from numerical integration. A number of studies [37, 38] thoroughly examine different numerical methods that are employed to treat this class of systems and classify such methods as either time-stepping or event-driven numerical integration. Contrary to any numerical integration scheme, the methodology of HSNC is not based on a stepwise evaluation of the sys-

tem and the response is computed in a vectorwise manner. The algorithm then only searches for dynamical switches in the obtained response that are known as events in the literature [37, 39]. In event-driven numerical integration, the methodology makes use of additional variables called event variables. Event variables are an indication of the active regime of motion (e.g., if the system is moving toward left or right in the case of Coulomb friction force) and are checked at every step. Upon an alteration in the event variables, an event is detected and the numerical solver switches to the appropriate governing equation of motion. The nature of such methods is still stepwise, and the event-driven algorithms are solely employed to increase the computational accuracy [35]. The only similarity between HSNC and event-driven numerical integration is in their search of events in their obtained response, which is an absolute necessity in treating any Filippov system regardless of the methodology.

Since HSNC uses an analytical approach in its response evaluation step, it is hundred to thousands of times faster than any numerical scheme while being as, if not more, accurate. In addition to the novelty and computational superiority of the current method relative to all its counterparts, its extendibility to all Filippov systems (that can be solved analytically in their intervals of continuity) is also an important characteristic of the methodology. Due to its computational efficiency, the methodology of this paper paves the way for real-time health monitoring of mechanical systems and enables a new more efficient analysis for many industrial applications.

To elucidate the HSNC method and to demonstrate its effectiveness, a number of PWLDFE systems are presented and analyzed in this paper. Although this work focuses on mechanical systems (i.e., a general mass-spring-damper plant with intermittent contact and Coulomb friction), it is important to note that the method is applicable to any PWLDFE system that can be analytically solved in its limited intervals of continuity.

The remainder of the paper is organized as follows. Section 2 is focused on introducing preliminary concepts and delineating the methodology. It primarily attempts to elucidate the problem and identify possible scenarios. Afterwards, it describes HSNC and its structure in detail. Section 3 presents a number of PWLDFE systems and demonstrates the effectiveness of HSNC. Section 4 concludes the paper and offers a discussion of the new method.

### 2 Methodology

The proposition of a standard mathematical formulation for PWLDFE systems is an essential step in efficient analysis and treatment of this class of nonlinear systems. Consequently, the first part of this section is primarily concerned with introducing a general formulation. It attempts to delineate the possible scenarios that can affect the PWLDFE systems' formulation. Since this paper is focused on mechanical systems, the general formulation of the PWLDFE systems takes the form of a general vibrating mechanical assembly. It should also be stated that the method works on

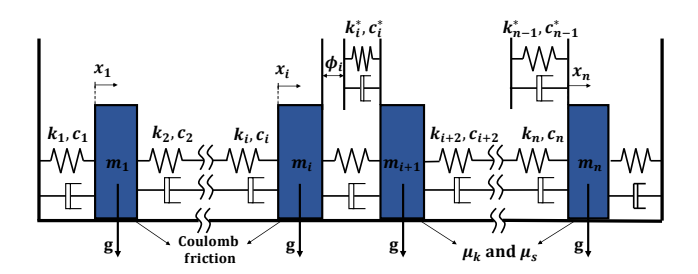


Fig. 1: Standard configuration of PWLDFE systems consisting of connected subsystems with intermittent contact

all other PWLDFE systems that can be solved analytically in their limited intervals of continuity.

Owing to the analytical nature of the proposed methodology and its reliance on the obtainment of a symbolic solution, it is essential to meticulously examine each regime of motion from a mathematical point of view and extract the cause and trigger of the dynamical switches (event). Consequently, a thorough discussion on the mathematics of vibrational systems with intermittent contact and Coulomb friction is offered in this section.

#### 2.1 Standard formulation of PWLDFE system

The standard formulation of the PWLDFE systems is presented in this subsection. Consider the nonlinear dynamics of a set of connected mass-spring-damper systems with intermittent contacts and Coulomb friction as depicted in Fig. 1.

The individual masses, addressed as subsystems in this work, can have intermittent contact with other subsystems. The contact pair consists of a spring and a damper that are proportionally related. The contact pairs can have contact or no contact depending on the system's position and will be further discussed in subsection 2.1.2. Equation (1) mathematically represents the general *n* degree-of-freedom (DOF) PWLDFE system as

$$\mathbf{M}\ddot{\mathbf{x}}(t) + \mathbf{C}\dot{\mathbf{x}}(t) + \mathbf{K}\mathbf{x}(t) - \mathbf{F}\sin(\omega t) \in \mathcal{D}(\mathbf{x}(t),\dot{\mathbf{x}}(t)),$$
 (1)

where  $\underline{\mathbf{x}}(t)$ ,  $\underline{\dot{\mathbf{x}}}(t)$  and  $\underline{\ddot{\mathbf{x}}}(t)$  are the position vector, velocity vector and acceleration vector, respectively;  $\mathbf{M}$ ,  $\mathbf{C}$  and  $\mathbf{K}$  represent the mass, damping and stiffness matrices, respectively; and  $\underline{\mathbf{F}}$  represents the magnitude of the excitation and  $\omega$  represents the frequency of excitation. The proportional damping also corresponds to the relation ( $\mathbf{C} = \beta \mathbf{K}$ ). The sign  $\in$  is the mathematical notation used to express differential inclusions and  $\mathcal{D}$  represents the collective mapping of all the discontinuous elements and consists of the multi-valued kinetic Coulomb friction vector, the multi-valued intermittent contact vector and the multi-valued staticity force vector. The nature and genesis of each of the aforementioned vectors will be discussed in detail in the coming subsections.

## 2.1.1 Multi-valued kinetic and static Coulomb friction force

The Coulomb friction causes the exertion of a multivalued force to each subsystem and the direction of this force is based on the subsystem's motion or direction of the static loads if the subsystem is stationary. Upon the movement of the subsystem, the value of this force is constant and its direction opposes motion. Alternatively, upon having staticity (when a subsystem sticks), the value of the Coulomb friction is equal in magnitude and opposite to the direction of the sum of all the acting forces until reaching the maximum static friction force. The kinetic multi-valued force vector, for the *j* subsystems in motion, can be mathematically expressed as

$$\mathcal{K}(\underline{\dot{\mathbf{x}}}(t)) = -\mu_k g \mathbf{M}_j \operatorname{sign}(\underline{\dot{\mathbf{x}}}_j(t)) = \begin{bmatrix} -\mu_k m_1 g \operatorname{sign}(\dot{x}_1(t)) \\ \vdots \\ -\mu_k m_j g \operatorname{sign}(\dot{x}_j(t)) \end{bmatrix} (2)$$

where  $\mu_k$  is the coefficient of kinetic friction and sign represents the sign function, and,  $\mathbf{M}_j$  and  $\dot{\mathbf{x}}_j$  represent the mass matrix and the velocity vector for the j moving subsystems. Upon encountering staticity in a subsystem, the kinetic Coulomb friction force changes to the static Coulomb friction as

$$S_i = |\text{Sum of all acting forces}| < \mu_s m_i g,$$
 (3)

where  $\mu_s$  represents the coefficient of static friction.

#### 2.1.2 Multi-valued intermittent contact force

The occurrence of intermittent contact alters the dynamics of the system and consequently affects the governing equation of motion as presented by Eq. (1). Before presenting a detailed discussion on the mathematical aspect of intermittent contacts, it is necessary to understand its behavior in depth. Assume that the  $i^{th}$  and  $(i+1)^{th}$  subsystems have intermittent contact. Then the two subsystem's intermittent contact pair has two distinct states (open or closed) and these states are contingent upon the numerical value of the *gap function*.

**Definition 1.** The gap function is used to determine the status of the intermittent contact of each contact pair. It can be mathematically represented as

$$G_i(t) = x_{i+1}(t) - x_i(t) + \phi_i,$$
 (4)

The status of each intermittent contact pair is contingent upon the position of the two engaged subsystems and the constant configuration parameter  $\phi$ . It must be noted that the constant parameter  $\phi$  is the distance from the  $i^{th}$  mass to the next adjacent intermittent contact pair when all the subsystems are in equilibrium. Next, the "open" and "closed" states will be defined for clarity.

**Definition 2.** The status of an intermittent contact pair is considered "open" if the value of the corresponding gap function is positive; the contact pair will then not experience contact and the intermittent contact pair's dynamics will not be involved in the dynamics. In contrast, if the value of the corresponding gap function is negative, then the intermittent contact pair's status is "closed", experiences contact, and henceforth is included in the dynamics. Figure 2 illustrates these two states.

To elucidate the mathematics of this subsection, let us assume that the system has one intermittent contact pair between the  $i^{th}$  and  $(i+1)^{th}$  subsystems. Initially, the intermittent contact pair's status is open, and therefore, the stiffness and damping associated with the contact are not involved in the dynamics of the system. Consequently, the defining matrices of the system are as initially defined by Eq. (1). After the change in status of the intermittent contact pair to "closed", the dynamics of the system changes and subsequently, the corresponding stiffness and damping matrices change. In other words, the involvement of the intermittent contact pair in the system's dynamics increases the stiffness and damping between the two subsystems. Mathematically speaking, matrices  $\bf C$  and  $\bf K$  change to

$$\mathbf{C}' = \mathbf{C} + \underbrace{\begin{bmatrix} \ddots & \vdots & \vdots & \vdots & \ddots \\ \ddots & \vdots & \vdots & \vdots & \vdots & \ddots \\ \vdots & \ddots & \vdots & \vdots & \ddots & \vdots \\ \ddots & \vdots & \vdots & \vdots & \ddots & \vdots \\ \ddots & \vdots & \vdots & \vdots & \vdots & \ddots & \vdots \\ \ddots & \vdots & \vdots & \vdots & \vdots & \ddots & \vdots \\ \ddots & \vdots & \vdots & \vdots & \vdots & \ddots & \vdots \\ \ddots & \vdots & \vdots & \vdots & \vdots & \ddots & \vdots \\ \ddots & \vdots & \vdots & \vdots & \vdots & \ddots & \vdots \\ \ddots & \vdots & \vdots & \vdots & \vdots & \ddots & \vdots \\ \lambda \mathbf{K}' = \mathbf{K} + \underbrace{\begin{bmatrix} \ddots & \vdots & \vdots & \vdots & \ddots & \vdots \\ \ddots & \vdots & \vdots & \vdots & \vdots & \ddots & \vdots \\ \ddots & \vdots & \vdots & \vdots & \vdots & \ddots & \vdots \\ \ddots & \vdots & \vdots & \vdots & \vdots & \ddots & \vdots \\ \ddots & \vdots & \vdots & \vdots & \vdots & \ddots & \vdots \\ \lambda \mathbf{K} \end{bmatrix}}_{\Delta \mathbf{K}}, \quad (5)$$

where the demonstrated rows and columns are related to the corresponding subsystems  $(i^{th})$  and  $(i+1)^{th}$  in this case), and  $k^*$  and  $c^*$  represent the spring stiffness and damping coefficient of the intermittent contact pair, respectively. It is noteworthy to state that only changing the  $\mathbf{C}$  and  $\mathbf{K}$  matrices does not fully capture the involvement of the intermittent contact pair in physical systems. In fact, as the intermittent contact pair engages, the spring force begins to rise from zero. However, the sole alteration of the  $\mathbf{K}$  matrix would induce a shock force that is not what would physically happen. To better explain this matter, consider expressing the intermittent contact pair's spring force as  $F_s$ 

$$F_s = \pm k^* \underbrace{(x_i(t) - x_{i+1}(t))}_{inconstant} - \underbrace{\phi_i}_{constant}). \tag{6}$$

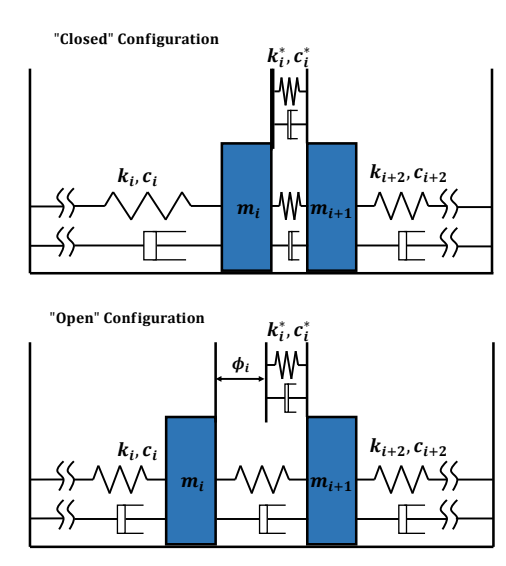


Fig. 2: Graphical representation of the two possible states of the intermittent contact pair

Equation (6) shows that the force can be separated into two parts that are fundamentally different. The first part is inconstant and is accounted for by changing the matrix **K**. In contrast, the second part is constant and its function is to make the spring force rise from zero as it physically does. This second part leads to the need to construct the constant part of the multi-valued intermittent contact force vector. If the status of the intermittent contact changes from open to closed, then the force vector that accounts for the constant part of the spring force is represented as

$$I = \left[ \cdots \left| -k^*(-\phi) \right| + k^*(-\phi) \right| \cdots \right]^T, \tag{7}$$

where the demonstrated elements are the  $i^{th}$  and  $(i+1)^{th}$ . Although one may think that a change in matrices  ${\bf C}$  and  ${\bf K}$ , in the left hand side of Eq. (1), is the better choice and is compatible with reality, to stay consistent with the mathematical notions of discontinuous mappings, these changes are made in the right hand side. That is, matrices  ${\bf C}$  and  ${\bf K}$  will never change directly and the left hand side of Eq. (1) remains single-valued throughout the occurrence of intermittent contact. Nonetheless, the multi-valued intermittent contact force will be constructed in a manner that resembles the change of Eq. (5). Mathematically speaking, the occurrence of intermittent contact can be presented as

$$\mathbf{M}\underline{\ddot{\mathbf{x}}}(t) + \mathbf{C}\underline{\dot{\mathbf{x}}}(t) + \mathbf{K}\underline{\mathbf{x}}(t) - \underline{\mathbf{F}}sin(\omega t) \in +I - \Delta\mathbf{C}\underline{\dot{\mathbf{x}}}(t) - \Delta\mathbf{K}\underline{\mathbf{x}}(t) + \mathcal{D}', \quad (8)$$

where  $\mathcal{D}'$  represents the other multi-valued force vectors (the multi-valued Coloumb friction in the context of the examples

of this paper). The collective effects of the mappings of Eq. (5,7) defines the occurrence of intermittent contact with precision as illustrated in Eq. (8).

**Remark 1.** It should be noted that the existence of the multi-valued force vectors  $(I, \Delta \mathbf{C} \dot{\mathbf{x}}(t))$  and  $\Delta \mathbf{K} \dot{\mathbf{x}}(t)$  depends on the status of the intermittent contact pairs. Eq. (8) illustrates the switch from open to closed. The switch from closed to open will translate into the elimination of the aforementioned vectors.

# 2.1.3 Staticity and the corresponding multi-valued force vector

The presence of Coulomb friction can cause the occurrence of the sticking phenomena. The sticking of a subsystem has the capability to alter all the defining matrices (mass, stiffness and damping) and also add constant forces to the new dynamics. This subsection is devoted to the detailed examination of the effects of the sticking of a subsystem on the vibration of PWLDFE systems.

Assume that the  $i^{th}$  subsystem's velocity reaches zero. This event means that the subsystem is no longer dynamic and to examine its motion, a force analysis is required. If the sum of all the acting forces on the static subsystem can overcome the maximum static Coulomb friction ( $\mu_s m_i g$ ), then the subsystem will only be instantaneously motionless and the subsystem will return to movement. Conversely, if the sum of all the acting forces on the static subsystem cannot overcome the maximum static Coulomb friction, then the subsystem sticks and remains static. This event, referred to as *staticity* in this paper, fundamentally alters the dynamics of the PWLDFE systems.

To mathematically formulate the effects of staticity, it is necessary to highlight its characteristics. The staticity of the  $i^{th}$  subsystem means that the  $i^{th}$  row and column of the governing equation of motion, which represents the dynamics of the  $i^{th}$  subsystem, must be eliminated. Nevertheless, the elimination of the  $i^{th}$  column that represents the effect of the  $i^{th}$  subsystem on the rest of the dynamics is not straightforward and the purely static  $i^{th}$  subsystem continues to affect the overall system dynamics. To elucidate this matter, it's beneficial to express the situation mathematically. In the case of staticity,  $\ddot{x}_i(t) = \dot{x}_i(t) = 0$  and this denotes that the acceleration and velocity of the static subsystem cannot affect the dynamics of the rest of the system. This can be verified by careful examination of Eq. (9).

$$F_{\text{damping}} = \begin{bmatrix} c_{11} & \cdots & c_{1i} & \cdots & c_{1n} \\ & \ddots & \vdots & \ddots & \\ \vdots & c_{ii} & \vdots & \vdots \\ & \ddots & \vdots & \ddots & \\ c_{n1} & \cdots & c_{ni} & \cdots & c_{nn} \end{bmatrix} \begin{bmatrix} \dot{x}_{1}(t) \\ \vdots \\ \dot{x}_{i}(t) = 0 \\ \vdots \\ \dot{x}_{n}(t) \end{bmatrix}$$

$$\xrightarrow{i^{th} \text{ subsystem's effect}} \begin{bmatrix} c_{1i} \\ \vdots \\ c_{ii} \\ \vdots \\ c_{ni} \end{bmatrix} \times \dot{x}_{i}(t), \quad (9)$$

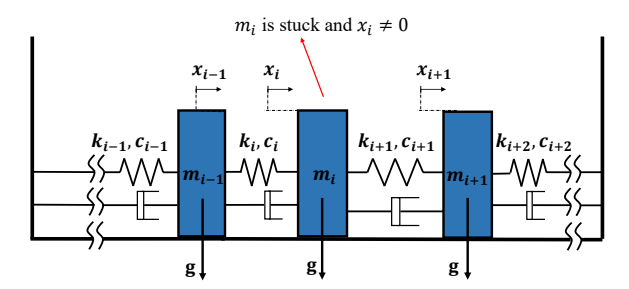
where the highlighted column corresponds to the  $i^{th}$  column and its multiplication by  $\dot{x}_i(t) = 0$  results in no damping forcing from the  $i^{th}$  subsystem due to its staticity. However,  $x_i(t) = constant$  and consequently, the multiplication of the elements of the  $i^{th}$  column of the stiffness matrix produces a nonzero force vector that affects the system's dynamics and cannot be neglected. Accordingly, and contrary to  $\ddot{x}_i(t)$  and  $\dot{x}_i(t)$ , the effects of the position of the static subsystem must be accounted for in the *new reduced dynamics*. This static forcing can be seen by inspecting Eq. (10) where the effect of the position of the  $i^{th}$  subsystem, on the rest of the dynamic system, is shown.

$$F_{\text{spring}} = \begin{bmatrix} k_{11} & \cdots & k_{1i} & \cdots & k_{1n} \\ & \ddots & \vdots & \ddots & \\ \vdots & & k_{ii} & & \vdots \\ & \ddots & \vdots & \ddots & \\ k_{n1} & \cdots & k_{ni} & \cdots & k_{nn} \end{bmatrix} \begin{bmatrix} x_{1}(t) & \vdots & \\ \vdots & \vdots & \vdots & \\ x_{i}(t) = constant & \vdots & \\ \vdots & \vdots & \vdots & \\ x_{n}(t) & \end{bmatrix}$$

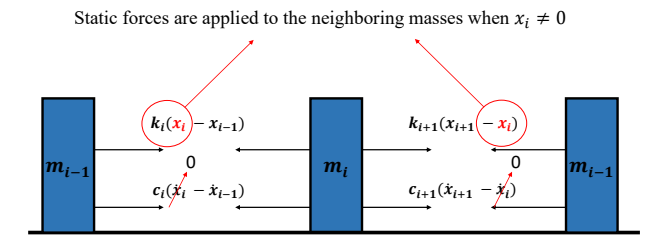
$$\xrightarrow{i^{th} \text{ subsystem's effect}} \begin{bmatrix} k_{1i} & \vdots & \\ \vdots & k_{ii} & \vdots & \\ k_{ni} & \vdots & \\ k_{ni} & \end{bmatrix}} \times x_{i}(t), \quad (10)$$

where  $F_{\text{spring}}$  represents the spring force vector of the dynamics. To further elucidate this effect, consider the specific portion of a PWLDFE system, represented by Fig. 3 where the  $i^{th}$  subsystem experiences staticity.

The static force results from the elongation or compression of the connecting springs in the adjacent subsystems. Note that no additional static forces result for the case where the  $i^{th}$  subsystem is stuck at  $x_i = 0$ . As the  $i^{th}$  row and column of the governing equation of motion must be eliminated when the  $i^{th}$  subsystem is stuck, a new constant force vector has to be added to take this into consideration. This elimination is due to the fact that that the  $i^{th}$  row describes the



(a) Mechanical view of the seperated section



(b) Only spring and damping force are illustrated

Fig. 3: The staticity of the  $i^{th}$  subsystem and the corresponding spring and damping forces

motion of the  $i^{th}$  subsystem. The corresponding multi-valued (yet constant) force vector can be defined as

$$S = -\begin{bmatrix} k_{1i} \cdots k_{(i-1)i} & k_{(i+1)i} \cdots k_{ni} \end{bmatrix}_{(n-1)\times 1}^{T} \times x_{i}.$$
 (11)

Note that the only difference between Eq. (11) and the separated section of Eq. (10) is in the elimination of the  $i^{th}$  row of Eq. (10). This elimination is done to account for the staticity of the  $i^{th}$  subsystem.

# 2.2 Switch definition, classification and detection2.2.1 Preliminary concepts and definitions

The previous subsections attempted to acquaint readers with the fundamentals of PWLDFE systems and express different events that can alter their formulation. These alternating events cause the discontinuities in the governing equation of motion and the multi-valued mapping  $\mathcal D$  is updated on the basis of their occurrence. An important step in understanding and efficient treatment of PWLDFE systems lies in the detection of these events. Before further advancement in this topic, it is necessary to provide a number of useful definitions.

**Remark 2.** A switch is defined as any event that causes a discontinuity in the governing equation of motion. Staticity, alteration of the direction of motion, and the change in the status of intermittent contact pairs are examples of switches for the systems considered in this work.

Switches can fundamentally alter the behavior of PWLDFE systems. Consequently, understanding their nature and corresponding effects facilitates the analysis and evaluation of PWLDFE systems. Next, the switches encountered in the PWLDFE systems presented in this work are discussed and classified.

**Definition 3.** Major switches form a class of switches that alter the underlying dynamical characteristics of the system such as natural frequencies or damping ratios. The major switches presented in this paper are triggered as a result of staticity or intermittent contact.

**Definition 4.** Minor switches form a class of switches that do not alter the dynamical characteristics of the system. The minor switches presented in this paper are triggered as a result of the change in the direction of motion (where no staticity occurs).

**Remark 3.** Minor switches do not alter the underlying dynamical characteristics of the system but this should not be confused with their capability to alter the dynamical behavior of the system, which they in fact do.

#### 2.2.2 Triggering conditions

The definition and classification of switches enables the discussion of triggering conditions and their effects on the governing equation of motion.

Kinetic Coulomb friction: This type of switch stems from an alteration in the direction of motion of a subsystem. Consequently, it is trivial that a change in the sign of the velocity can be interpreted as the requirement for the occurrence of this type of switch. Mathematically speaking, the condition to trigger this switch is

$$\dot{x}_i(k+1) \times \dot{x}_i(k) < 0$$
 and  $|\text{sum of acting forces on } i^{th} \text{ subsystem}| > \mu_s m_i g, \quad (12)$ 

where k represents the  $k^{th}$  step in time. It is important to note that the sole occurrence of the first part of Eq. (12) does not necessarily result in a switch of this kind and as discussed previously, a force analysis is required. If the subsystem that reaches zero velocity jumps out of it instantaneously, then the switch is of this kind. Otherwise, the switch is causing staticity. The sole effect of this switch on the system is causing a change in the sign of the kinetic Coulomb friction force because this force is defined as  $-sign(\dot{x}_i)\mu_k m_i g$ . Although this change seems small, it should be noted that it can affect the general behavior of the system and impair the employment of numerous techniques.

Intermittent contact: This type of switch stems from the alteration of the status of an intermittent contact pair. To check for the occurrence of switches that are related to intermittent contact pairs, it is only necessary to monitor their corresponding gap function, as defined by Eq. (4). A change in the sign of the gap function results in a change in the status of the intermittent contact pair.

To mathematically formulate the triggering condition of this switch, it can be said that

$$G_i(k+1) \times G_i(k) < 0, \tag{13}$$

which indicates the sign of the gap function has changed.

Staticity: This type of switch stems from the sticking of a subsystem due to static Coulomb friction. The detection of this type of switch is similar to "kinetic Coulomb friction". A change in the sign of the velocity of the  $i^{th}$  subsystem means that the subsystem's velocity has reached zero. At this point, it is necessary to conduct a force analysis and if the sum of all acting forces on the  $i^{th}$  subsystem cannot overcome the maximum static Coulomb friction, then this type of switch has occurred. Mathematically speaking, if

$$\dot{x}_i(k+1) \times \dot{x}_i(k) < 0$$
 and  $|\text{sum of acting forces on } i^{th} \text{ subsystem}| \le \mu_s m_i g$ , (14)

then the *i*<sup>th</sup> subsystem sticks and the dynamics is altered as discussed in subsection 2.1.3. It is important to note that the stuck subsystem, which is eliminated from the dynamic equations, should not be forgotten and must be continuously monitored to see if the sum of all acting forces on that subsystem overcome the maximum static Coulomb friction. In that case, the corresponding constant force vectors must be eliminated and the deleted *i*<sup>th</sup> row (and column) must be restored.

The triggering conditions and corresponding effects of the switches on the governing equation of motion has been carefully studied in this section. Now, it is possible to discuss HSNC in detail and how it can be used to evaluate responses of PWLDFE systems.

#### **2.3 HSNC**

#### 2.3.1 Fundamentals of HSNC

Before delving into the detailed mathematical structure of HSNC, it is beneficial to present a brief overall picture. As discussed in the previous section, it can be observed that, apart from the constant force vectors, the equations of motion are linear at all times. That is, the equations of motion can be presented by single-valued linear differential equations (with constant forces) until a switch occurs. The occurrence of a switch alters the equation of motion but the new equation of motion can again be presented by another single-valued linear differential equation (with constant forces that will differ from the previous case). In fact, the differential inclusion can be thought of as a number of different differential equations that are stitched together. HSNC exploits this property and its foundation is based on the fact that the problem can be reformulated as a number of linear differential equations that produce a continuous response despite being discontinuous themselves. It initially manipulates the starting differential equation of motion to cast it into a fully linear formulation. Then, it applies modal transformation and decouples the coupled dynamics to facilitate the analytical solving of the set of differential equations. It then, obtains the response of the system. It is critical to bear in mind that the obtained results are valid until the occurrence of the earliest switch. This is because after the occurrence of the earliest switch,

the governing equations of motion are no longer valid and the multi-valued mappings (right-hand side) of the equations of motion will change. It is important to note that the HSNC method can incorporate multiple numerical techniques to increase its computational efficiency. Consequently, a hybrid numerical analytical method is obtained. The following subsections will detail each part of this algorithm.

#### 2.3.2 Temporary disposable coordinates

As stated in the previous subsection, the first step is to cast the differential equations with constant force vectors into a fully linear formulation. This casting process should be performed for the time interval in which the governing equation of motion remains continuous and no switches occur. To perform this casting process, in the limited time interval, it is beneficial to mathematically manipulate the differential equation to remove the constant forces. This can be done by introducing a new set of coordinates. The intention of this set of coordinates is to eliminate the constant force vectors upon substitution. Consequently, the new temporary set of coordinates is defined as  $\underline{\mathbf{x}}'(t) = \underline{\mathbf{x}}(t) - \boldsymbol{\gamma}$  where  $\boldsymbol{\gamma}$  is determined based on the mapping  $\mathcal{D}$ . Depending on the status and velocity of the subsystems, the value of the  $\gamma$  vector can have numerous distinct values. The mathematical definition of  $\gamma$  can be stated as

$$\mathbf{\gamma} = \mathbf{K}^{-1} \times \mathcal{D}. \tag{15}$$

Utilizing  $\gamma$  and the newly defined coordinates, it is possible to reduce the general formulation of Eq. (1) to

$$\mathbf{M}\ddot{\mathbf{x}}'(t) + \mathbf{C}\dot{\mathbf{x}}'(t) + \mathbf{K}\mathbf{x}'(t) - \mathbf{F}\sin(\omega t) = 0.$$
 (16)

Equation (16) is fully linear and allows a modal transformation to decouple the coupled equations of motion. The modal coordinate is proposed as  $\underline{\mathbf{x}}'(t) = \psi \underline{\mathbf{q}}(t)$  with respect to the literature [40]. By applying the modal coordinates to Eq. (16), the decoupled differential equations will be obtained as

$$\mathbf{\psi}^{T}\mathbf{M}\mathbf{\psi}\ddot{\mathbf{q}}(t) + \mathbf{\psi}^{T}\mathbf{C}\mathbf{\psi}\dot{\mathbf{q}}(t) + \mathbf{\psi}^{T}\mathbf{K}\mathbf{\psi}\mathbf{q}(t) = \mathbf{\psi}^{T}\underline{\mathbf{F}}\sin(\omega t), (17)$$

Or alternatively as

$$\ddot{q}_i(t) + 2\xi_i \omega_{n_i} \dot{q}_i(t) + \omega_{n_i}^2 q_i(t) = f_i \sin(\omega t), \quad i = 1, \dots, n.$$
(18)

Note that the damping matrix  $\mathbf{C}$  is diagonalizable using the modal transformation if the system is proportionally damped and the decoupled differential equations can now be solved analytically and the response is obtained in modal coordinates. The response can then be transformed back to the original physical coordinate  $\underline{\mathbf{x}}(t)$  by using the relation  $\underline{\mathbf{x}}'(t) = \psi \underline{\mathbf{q}}(t)$  and  $\underline{\mathbf{x}}'(t) = \underline{\mathbf{x}}(t) - \gamma$ . It is important to note that the obtained response is valid up to the occurrence of the earliest

switch. Consequently, the next step consists of checking for the occurrence of a switch.

As discussed in subsection 2.3.1, the HSNC algorithm consists of stitching the obtained responses together. To follow this procedure, it is necessary to present the final value of the current interval (which is the point where the earliest switch occurs) as the initial value of the next interval.

#### 2.3.3 Switch detection

The next part of the HSNC algorithm consists of finding the earliest switch. The triggering conditions of all switches has been discussed in subsection 2.2 and it is only necessary to check for their occurrence. This can be done by evaluating the response of the system up to a rational predetermined value (the period of excitation can be considered as an adequate choice). All the triggering conditions (subsystem's velocities, gap functions and force analysis of static subsystems) of every subsystem must then be assessed and the earliest switch must be identified. The time that corresponds to this switch, referred to as the critical switch, must be extracted and the response of the system, up to that point, must be stored as the response up until the critical switch. The rest of the obtained response should be discarded since the occurrence of the critical switch will alter the dynamics and the mapping  $\mathcal{D}$ .

**Remark 4.** An additional reason for separating the switches into major and minor becomes apparent in the detection step. To check for the occurrence of major switches it is necessary to reconstruct the initial physical coordinates  $(\underline{\mathbf{x}}(t))$  but minor switches can be detected directly in modal coordinates.

## 2.3.4 Detection mechanism and the critical subsystem tracker

The detection of the switches is achieved by obtaining the response of the system and assessing the triggering conditions. Contrary to NI methods, this response obtainment is not executed in a stepwise manner but using a vectorwise approach. This vectorwise evaluation is the fundamental computational advantage of the HSNC algorithm. Nonetheless, the step size of the utilized time vector dictates the accuracy of finding the location of the critical switch. The idea of choosing an extremely small step size can be dismissed since it imposes a heavy computational burden to the processing unit and undermines one of the fundamental advantages of HSNC. However, large step sizes can result in the missing of switches and result in an erroneous critical switch detection.

To overcome these competing issues, it is possible to interlace the analytical structure of the HSNC with efficient numerical methods. HSNC can be used to identify the location of the critical switch between two consecutive steps. Figure 4 illustrates this matter and considers the gap function of a subsystem to be of interest. Once the region where the critical switch occurs has been identified, it is possible to the employ a numerical nonlinear solver to identify the precise time of the critical switch. The simulations in this work employed MATLAB's *fzero* nonlinear solver to acquire the

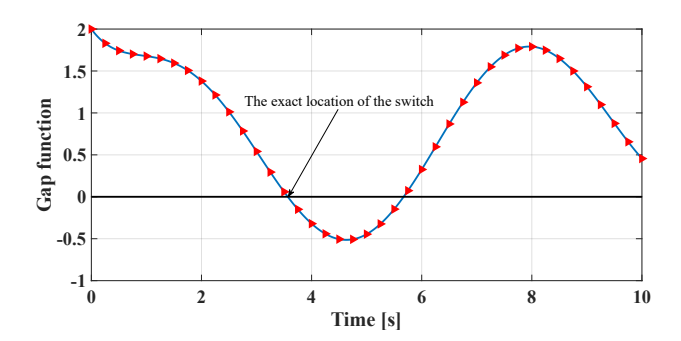


Fig. 4: The solid line corresponds to the gap function and the red triangles indicate the evaluted points; the switch occurs when the gap function changes sign and is placed between two points

precise location of the critical switch since this solver is fast and reliable. The *fzero* nonlinear solver also uses the upper and lower bounds for solving the exact transition time, which is readily computed by HSNC. Nonetheless, HSNC does not limit the users to any specific nonlinear solver and alternative solvers can also be employed with HSNC.

The addition of the nonlinear solver to the structure of HSNC engenders certain issues, and if not properly managed, can cause its systematic failure. The issue with the nonlinear solver lies in its numerical nature. When a subsystem causes a critical switch (let us assume an intermittent contact), the value of the function that corresponds to its triggering condition (gap function in this example) should be equal to zero at that precise instant. Nevertheless, due to the numerical nature of the nonlinear solver, the obtained value for the critical switch's time corresponds to a near zero value for that function ( $\pm \epsilon$  where  $\epsilon$  represents a very small value) and not exactly zero. Since the triggering conditions depend solely on sign changes, the fact that the value of the triggering function that corresponds to the subsystem that experienced the critical switch does not equal exactly zero at the first step of the next iteration can cause false switch detections. To elucidate this matter, assume that a subsystem experiences an intermittent contact and its status changes from closed to open. The value of the corresponding gap function at the first step of the next iteration should be equal to zero, but, due to the numerical nature of the nonlinear solver, this value is obtained to be  $-10^{-15}$ . As the system is now open, the value of the second step of the corresponding gap function will be positive. The algorithm will then detect that a sign change has occurred between the first and second step of this gap function and this fact translates into the occurrence of another switch. However, this is a false detection and consequently, this issue should be resolved.

To overcome this issue, the *critical subsystem tracker* mechanism was introduced. The underlying idea of this mechanism is to track the subsystem that experiences the critical switch and to automatically equate the first step of the triggering function that experienced the critical switch in its previous iteration to zero in the subsequent iteration. In fact, this method rectifies the numerical error of the nonlin-

ear solver and prevents the HSNC algorithm from detecting false switches.

Note that upon finding any switch, the final point of the time vector is changed from their predetermined value to the earliest switch found. The logic behind this idea is to tighten the search space because, as stated previously, the rest of the data are incorrect since they employ the inaccurate equations of motion.

The final point that might appear ambiguous to the readers is the significant difference between NI methods' runtime and HSNC's. There exist two fundamental causes for this matter and the first one is the dependency of NI's accuracy on the selected time step. In many cases of PWLDFE systems, the selection of a large (or in some cases, even relatively small) time steps results in the failure of the NI method in capturing the entirety of the system's dynamics and consequently, excessively small time steps are required. In contrast, this is never the case in HSNC and the time step's size can be quite large. This is due to the fact that HSNC searches for switches and does not evaluate the response in a stepwise manner. The second reason is that NI methods are required to calculate each step after the previous one but HSNC allows the vectorwise evaluation of the response since the analytical solution is used. Figure 5 illustrates the overall structure of the HSNC algorithm.

#### 3 Results and discussion

Results of employing the HSNC algorithm for two different mechanical assemblies are simulated and presented in this section. The presented systems are of interest for a number of reasons. First, the assembly can be used as a model for a wide range of industrial applications. Second, by tuning the parameters, it is possible to obtain weakly chaotic responses. Such a motion is very rarely encountered in nonlinear dynamics and therefore, requires attention and special care. Finally, the second assembly of this section is a high dimensional system and is presented here to further illustrate the capabilities of HSNC. High dimensional mechanical assemblies with piecewise linear nonlinearities and Coulomb friction are frequently seen in turbomachinery applications and due to their complexity and high dimensionality, new efficient tools to handle PWL systems are needed.

#### 3.1 Two DOF mechanical system

The first system consists of a two DOF mass-springdamper system with intermittent contact between the two masses and Coulomb friction as depicted in Fig. 6.

This system is simulated for three different scenarios. The system is harmonically excited and the parameters, for all scenarios, are presented in Table 1.

The first scenario is selected to illustrate the effectiveness of HSNC relative to NI methods when the system has a conventional periodic response. The NI method of this work is the fourth order Adams-Bashforth method that is known for its accuracy and stability. Figure 7 illustrates the response of the system.

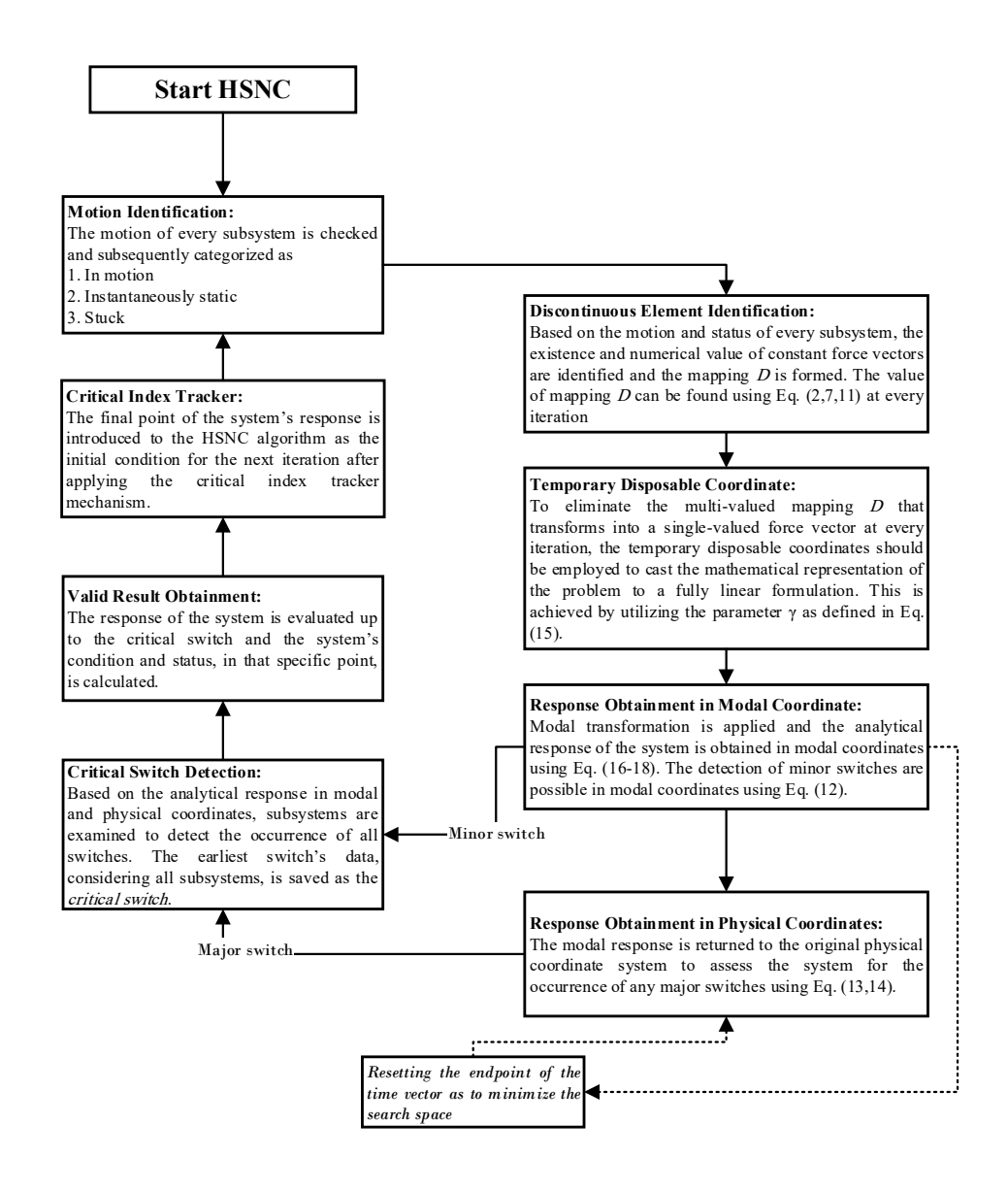


Fig. 5: Overview of the HSNC algorithm

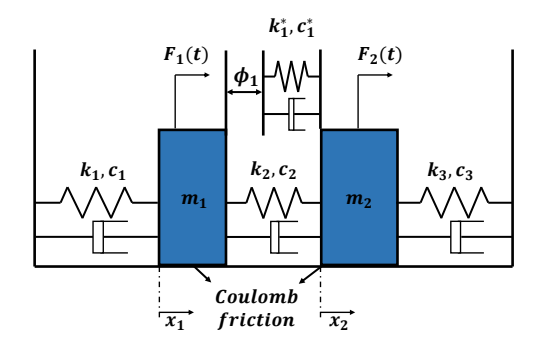


Fig. 6: Two DOF PWLDFE system

Both methods obtain very similar responses for each mass, which verifies the accuracy of HSNC with a traditional

NI method; however, the difference between their computational costs are considerable. The runtime of HSNC is about **1766 times** faster than NI. The exact runtime of each method for all of the scenarios is presented in Table 2.

It is important to note that NI's time step size was selected to be  $h=10^{-6}$  to produce accurate results. It is evident that despite its better computational efficiency, the results of HSNC are more reliable due to its analytical nature. To emphasize the accuracy of HSNC, the parameters of the system from scenario 2 are used. This simulation demonstrates the effectiveness of HSNC in treating systems where NI methods struggle with conventional time step sizes. The system is solved via NI with two different time steps and the results illustrate a significant difference. The results of HSNC match with the results of the NI method with the smaller time step.

The response obtained via the NI method demonstrates

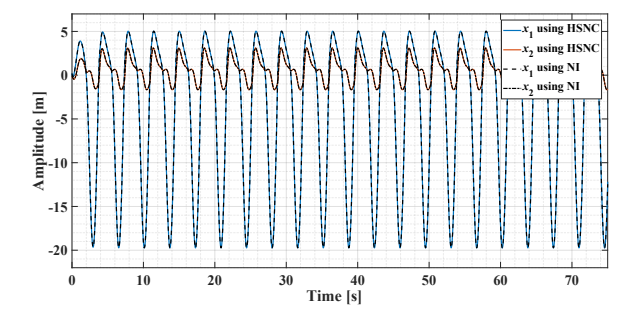


Fig. 7: Time evaluation of the 2-DOF system with first scenario parameters

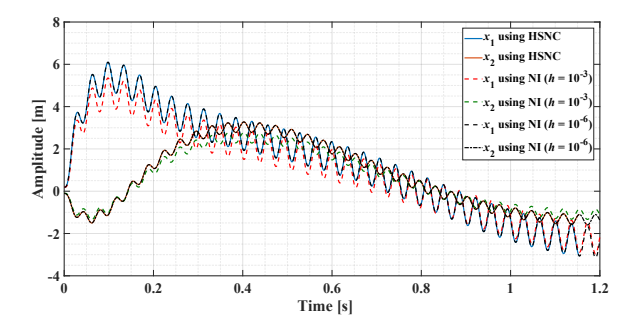
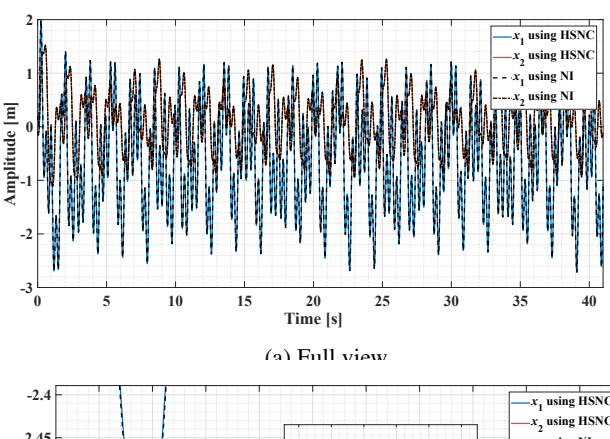


Fig. 8: Time evaluation of the 2-DOF system with second scenario parameters and the comparison of the obtained results

significant error when the time step is selected to be a conventional value ( $h = 10^{-3}$ ) and a much smaller time step is required to obtain the response with acceptable accuracy ( $h = 10^{-6}$ ). The runtime of the methods are also compared and it is observed that the HSNC is about **45 times** faster for this scenario.

**Remark 5.** The significant difference between the performances of HSNC in the previous scenarios might puzzle the readers since, in the first scenario, the HSNC is about 1766 times faster but in the second case it is only 45 times faster. To understand this, the structure of HSNC must be revisited in detail. As discussed in subsection 2.3.4, the response of the system is obtained via an analytical solution and a critical switch detection algorithm. A significant decrease in the distance between switches results in an increase in the number of response evaluations and a multitude of changes in the governing equation of motion. This phenomenon pushes the nature of HSNC from a vectorwise algorithm to a semi stepwise algorithm since the consecutive switches are very close. This causes an increase in the runtime of HSNC but it is critical to state that even in such a case, HSNC is much faster.

An alternative point that should be noted from the previous simulation is the challenges placed on NI methods in treating PWLDFE systems. The mathematical representation of PWLDFE systems is swarmed with *switches* and the detection of such switches using NI methods, that employ a stepwise evaluation scheme, is intertwined with algorithmic



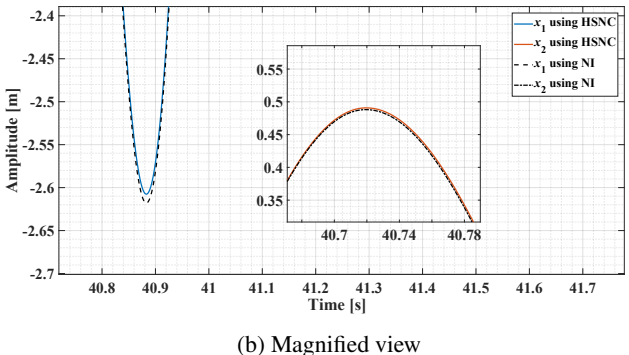


Fig. 9: The weakly chaotic response of the PWLDFE system

and computational difficulties. Consequently, even for the simple case of this simulation, the NI methods exhibit their fundamental drawbacks.

The third scenario is meant to illustrate the weakly chaotic motion that can be obtained in PWLDFE systems.

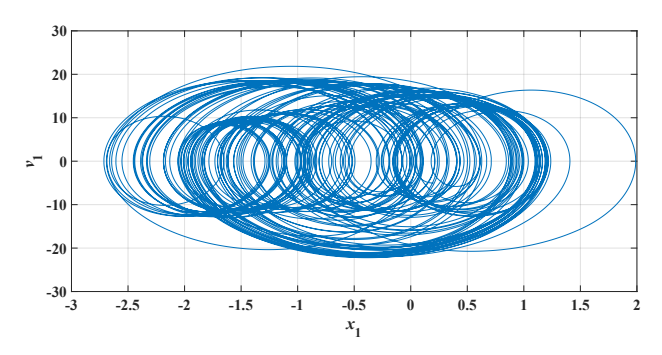
As demonstrated in Fig. 9, the motion of the system is not periodic and seems to be chaotic. The phase portrait of the system indicates the existence of a strange attractor as presented by Fig. 10 and the system does not settle at any trajectories. The runtime of the HSNC is about **432 times** faster in this case.

Nonetheless, as illustrated in Fig. 11, the divergence of two infinitesimally close trajectories is not exponential at all and the trajectories seem to diverge very slowly. The initial distance between the initial values (the position of the second mass only) is  $\delta = 10^{-3}$ . Such weakly chaotic motions have not been reported in mechanical systems prior to this research and were limited to a very specific class of motions [41]. The slow divergence of two infinitesimally close trajectories is also demonstrated in the phase plane in Fig. 12.

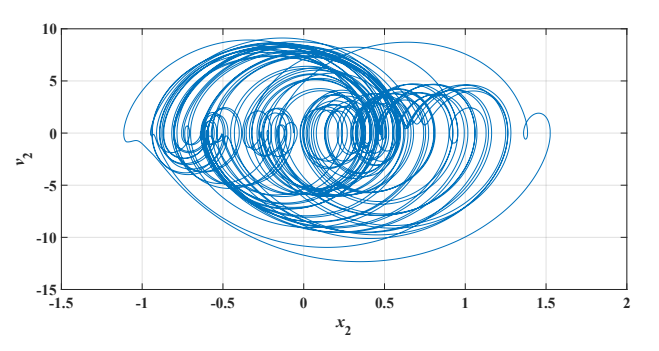
An interesting discussion can be held on the accuracy of HSNC relative to NI methods for the case of weakly chaotic motions. It is evident that due to the reliance of both methods to numerical techniques, the response of both methods will diverge from the true response in infinite time. Nonetheless, the dependency of NI methods on numerical methods occurs in a stepwise manner and at each step, a numerical error is added that will accelerate the divergence from the true response. In contrast, HSNC's only source of numerical error

Table 1: The numerical value of the first simulated system for all scenarios

Scenario	$m_1$	$m_2$	$k_1$	$k_2$	$k_3$	β	$\mu_k$	$\mu_{\scriptscriptstyle S}$	$F_1$	$F_2$	ω	$k^*$	$\phi_1$
1	1	2	5	10	40	0.1	0.6	0.75	225	-150	1.75515	100	0.2
2	1	2	5	10	40	0.1	0.6	0.75	22500	-15000	175.5151	100	0.2
3	1	2	5	10	40	0	0.6	0.75	225	150	17.5515	100	0.2



(a) The phase portrait of the first subsystem and its weakly chaoti motion



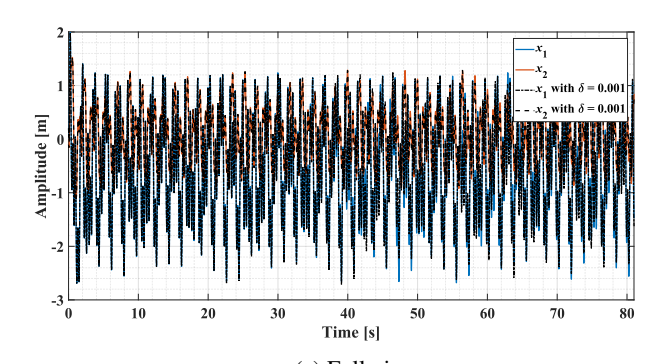
(b) The phase portrait of the second subsystem and its weakly chaotic motion

Fig. 10: The phase portrait of the third scenario and its weakly chaotic motion

is in the exact identification of the switch's time when in this work it employs the *fzero* solver. Consequently, the response of HSNC, in the case of weakly chaotic motion is closer to the true response for an extended amount of time and subsequently, its accuracy is superior to NI methods *regardless* of their time step size. This higher accuracy is in addition to the fact that HSNC is considerably faster.

## 3.2 High dimensional mechanical system

The second system of interest is a higher dimensional mechanical system with intermittent contacts and Coulomb friction. Higher dimensional mechanical systems with a large number of nonlinearities are common in engineered structures such as turbomachinery, which have a number of



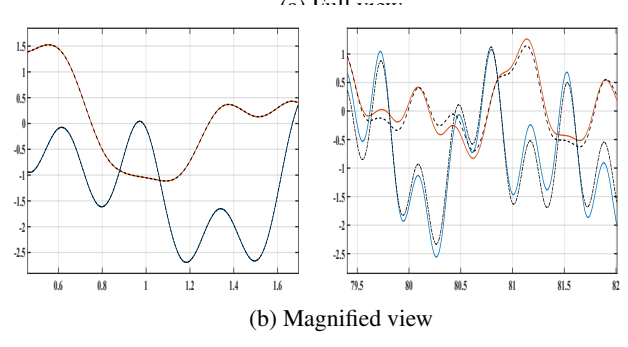


Fig. 11: The slow divergence of two infinitesimally close trajectories for weakly chaotic motion; the trajectories are very close at the beginning and start to diverge non-exponentially

different damping technologies that are often incorporated based on friction damping [42–45]. These systems are often exceedingly complex and use a number of reduction techniques to handle small and large mistuning [46, 47], aeroelastic effects [48], multistage rotors [49], rotational speed effects [50], and nonlinearity [50]. The system discussed in this section is not as large as these very high dimensional systems; however many of the model reduction methods that are used to lower the dimensionality of the linear degrees of freedom can be integrated with HSNC in a similar manner to how BAA was integrated with turbomachinery [26, 51]. Therefore this example is focused on demonstrating how the method can effectively analyze a system with a large number of connected nonlinearities with each degree of freedom having Coulomb friction as well as having multiple intermittent contact pairs.

The system under study is a 34-DOF mass-spring system with Coulomb friction and multiple intermittent con-

Table 2: Runtime comparison of HSNC with NI for simulated systems

Runtime [s]	Scenario 1	Scenario 2	Scenario 3	High Dimensional
HSNC	0.600	0.462	1.382	10.03
NI	1059	20.85	597.5	2333

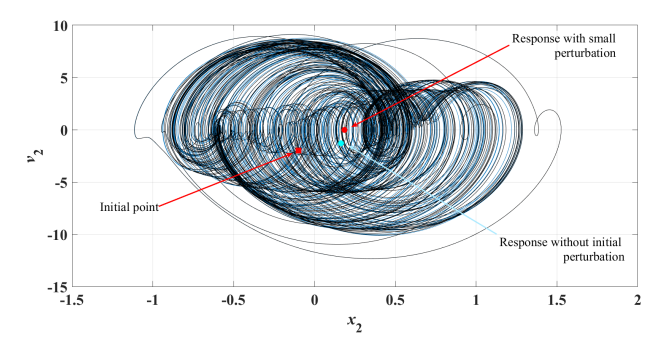


Fig. 12: Non-exponential trajectory divergence in weakly chaotic motion

tacts. The corresponding numerical values of this system's parameters are presented in Appendix A for convenience. Figure 13 illustrates the response obtained using HSNC and NI and demonstrates the accuracy of HSNC. The runtime of HSNC is also about **232 times** faster in this scenario and the runtime, for each method, is presented in Table 2. Note that this is a very complex scenario where many stick slip transitions can occur in rapid succession.

#### 3.3 Limitations

Despite the noted advantages, the presented methodology of this paper is constrained in use by certain limitations. Primarily, HSNC can only be used for PWLDFE systems that can be solved analytically in their intervals of continuity. Since a major class of models in mechanical vibration are linear or can be adequately approximated by linear or piecewise linear components, the applicability of this methodology is widely preserved. Nevertheless, for heavily nonlinear systems with inherently nonlinear components, the attainment of an analytical solution is not possible and consequently, the employment of HSNC will be impossible.

The second major limitation of the proposed HSNC lies in its inability to treat continuous systems that form an alternative class of vibrational systems. Bear in mind that HSNC relies on using analytical solutions of ODEs in their intervals of validity to compute the response of the system. In contrast, continuous systems are modeled via partial differential equations (PDEs) and are therefore fundamentally different. Nevertheless, it is possible to extend the concepts of HSNC to continuous systems by applying the same principles to PDEs. However, since the analytical solutions of PDEs are

even harder to obtain, the complexity of the methodology will increase significantly.

### 3.4 Potential Applications

It is beneficial to further discuss the real-world applications of HSNC. The applications of this new methodology, apart from introducing a new computationally superior approach, lie within the speedy evaluation of engineering systems. The dynamics of many engineering systems, from civil structures to turbomachinery equipment, are known to be best modeled via PWLDFE systems. In numerous cases, these systems have to be constantly monitored to ensure their structural health. Study [52] discusses several different approaches in the structural health monitoring of systems. Interestingly, a key component of monitoring the behavior of a healthy structure is the capability to predict the motion of the structure in different circumstances and identify mistuning [53] or irregularities (such as cracks) [36, 54] in a fast manner. In this case, the computational efficiency and speed of HSNC can considerably improve the quality of the monitoring system and avoid possible damage. Study [12] explores the validity of this class of solvers experimentally and verifies their accuracy and applicability.

#### 4 Conclusion

This paper primarily discusses systems that are piecewise linear with discontinuous force elements (PWLDFE) as accurate models for numerous physical phenomena and then offers a standard formulation and analysis tool for such models. The mathematics of the PWLDFE systems are discussed in detail for systems with intermittent contact and Coulomb friction and all of its variations are studied and classified. The PWLDFE systems are not only important from an industrial point of view, but also bear scientific significance. They are known to model the behavior of numerous real world systems and also demonstrate a wide range of motions. The weakly chaotic motion is observed in the response of PWLDFE systems and this type of motion has never been reported in mechanical assemblies before. In addition to a thorough examination of the mathematics of such systems, a novel efficient hybrid symbolic-numeric computational (HSNC) method is presented that is capable of obtaining the total response of this class of systems efficiently and accurately. The new method highlights its advantage in both simple and complex nonlinear systems, and can be read-

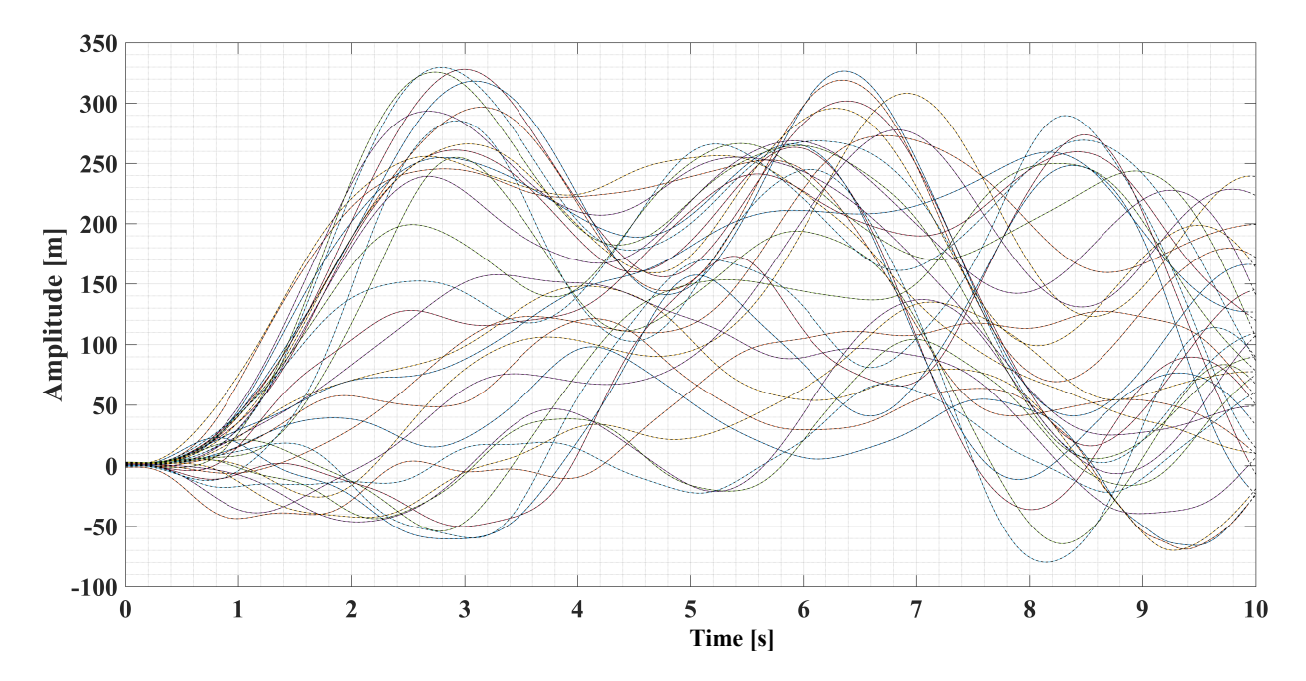


Fig. 13: Response of the High dimensional system obtained via both HSNC and NI; solid color lines indicate HSNC's response while dashed blacked lines are NI's response

ily combined with a number of model reduction techniques to handle high dimensional complex nonlinear systems, such as those found in turbomachinery. In addition to its speed, HSNC is also very accurate since it employs an analytical approach in obtaining the response of the system.

### 5 Acknowledgment

This paper is based on work partially supported by the National Science Foundation (United States) under Grant No. 1902408, program manager Dr. Harry Dankowicz, and the Ministry of Science and Technology (Taiwan, R.O.C) under Grant No. MOST 109-2222-E-007-006-MY3. Any opinions, findings, and conclusions or recommendations expressed in this paper are those of the authors and do not necessarily reflect the views of the National Science Foundation and the Ministry of Science and Technology.

# A Numerical values of the high dimensional system's parameters

Parameter	Value	Parameter	Value	Parameter	Value	Parameter	Value
$k_1$	10	k <sub>29</sub>	18	$m_{22}$	1.97	$F_{16}$	300
$k_2$	20	k <sub>30</sub>	15	$m_{23}$	2.2	$F_{17}$	240
$k_3$	15	k <sub>31</sub>	17	$m_{24}$	2.5	$F_{18}$	150
$k_4$	20	$k_{32}$	16	$m_{25}$	1.93	$F_{19}$	300
$k_5$	10	k <sub>33</sub>	20	$m_{26}$	1.82	$F_{20}$	450
$k_6$	21	k <sub>34</sub>	21	$m_{27}$	1.35	$F_{21}$	-300
$k_7$	13	k <sub>35</sub>	18.5	$m_{28}$	1.6	$F_{22}$	600
$k_8$	24	$m_1$	1	$m_{29}$	1.9	$F_{23}$	-300
$k_9$	20	$m_2$	1.1	$m_{30}$	1.4	$F_{24}$	285
$k_{10}$	21	$m_3$	2	$m_{31}$	2.2	$F_{25}$	-750
$k_{11}$	23	$m_4$	1.5	$m_{32}$	3.2	$F_{26}$	450
$k_{12}$	24	$m_5$	1.6	$m_{33}$	1.3	$F_{27}$	150
$k_{13}$	25	$m_6$	1.4	$m_{34}$	1.2	$F_{28}$	-600
$k_{14}$	13	$m_7$	2.3	$F_1$	300	$F_{29}$	1050
k <sub>15</sub>	16	$m_8$	2.5	$F_2$	-150	$F_{30}$	-1200
k <sub>16</sub>	17	<i>m</i> 9	1.9	$F_3$	225	$F_{31}$	300
$k_{17}$	18	$m_{10}$	1.5	$F_4$	210	$F_{32}$	-300
$k_{18}$	14	$m_{11}$	1.8	$F_5$	300	$F_{33}$	450
$k_{19}$	15	$m_{12}$	1.3	$F_6$	-525	$F_{34}$	-600
$k_{20}$	13	$m_{13}$	1.54	$F_7$	600	$\mu_k$	0.6
$k_{21}$	12	$m_{14}$	1.8	$F_8$	300	$\mu_s$	0.75
$k_{22}$	15	$m_{15}$	1.7	$F_9$	525	ω	1.7552
$k_{23}$	12	$m_{16}$	1.5	$F_{10}$	900	g	9.81
k <sub>24</sub>	14	$m_{17}$	1.9	$F_{11}$	300	β	0
$k_{25}$	10	$m_{18}$	1.6	$F_{12}$	-270		
$k_{26}$	14	$m_{19}$	1.5	$F_{13}$	300		
$k_{27}$	10	$m_{20}$	1.5	$F_{14}$	360		
$k_{28}$	13	$m_{21}$	1.17	$F_{15}$	300		

Note that  $k_i$  represents the spring that connects the  $(i-1)^{th}$  mass to the  $i^{th}$  mass;  $m_i$  represents the mass of the  $i^{th}$  subsystem;  $F_i$  corresponds to the excitation force acting on the  $i^{th}$  mass;  $\omega$  represents the excitation frequency; and  $\beta$  is the proportionality ratio for the damping. All units are in S.I.. The first and the second mass and also the second and the third mass have intermittent contact and the corresponding values of the intermittent contact pairs are given in the following table.

Parameter	Value
$k_1^*$	100
$k_2^*$	50
$\phi_1$	0.2
$\phi_2$	0.5

#### References

- [1] Mitra, M., and Epureanu, B. I., 2019. "Dynamic modeling and projection-based reduction methods for bladed disks with nonlinear frictional and intermittent contact interfaces". *Applied Mechanics Reviews*, **71**(5).
- [2] Öktem, H., 2005. "A survey on piecewise-linear models of regulatory dynamical systems". *Nonlinear Analysis: Theory, Methods & Applications*, **63**(3), pp. 336–349.
- [3] Zucca, S., and Epureanu, B. I., 2018. "Reduced order models for nonlinear dynamic analysis of structures with intermittent contacts". *Journal of Vibration and Control*, **24**(12), pp. 2591–2604.
- [4] Zucca, S., and Epureanu, B., 2014. "Bi-linear reducedorder models of structures with friction intermittent contacts". *Nonlinear Dynamics*, 77(3), pp. 1055–1067.
- [5] Kim, Y. B., and Noah, S. T., 1991. "Stability and Bifurcation Analysis of Oscillators With Piecewise-Linear Characteristics: A General Approach". *Journal of Applied Mechanics*, 58(2), 06, pp. 545–553.
- [6] Pasternak, E., Dyskin, A., and Qi, C., 2020. "Shifted impact oscillator: Tuned multiple resonances and step load". *International Journal of Engineering Science*, 147, p. 103203.
- [7] Guzek, A., Dyskin, A. V., Pasternak, E., and Shufrin, I., 2016. "Asymptotic analysis of bilinear oscillators with preload". *International Journal of Engineering Science*, 106, pp. 125–141.
- [8] Li, Z., Ouyang, H., and Guan, Z., 2017. "Friction-induced vibration of an elastic disc and a moving slider with separation and reattachment". *Nonlinear Dynamics*, **87**(2), pp. 1045–1067.
- [9] Marton, L., and Lantos, B., 2007. "Modeling, identification, and compensation of stick-slip friction". *IEEE Transactions on Industrial Electronics*, **54**(1), pp. 511–521.
- [10] Natsiavas, S., 1998. "Stability of piecewise linear oscillators with viscous and dry friction damping". *Journal of Sound and Vibration*, **217**(3), pp. 507–522.
- [11] Li, Y., and Feng, Z., 2004. "Bifurcation and chaos in friction-induced vibration". *Communications in Nonlinear Science and Numerical Simulation*, **9**(6), pp. 633–647.
- [12] Saito, A., Umemoto, J., Noguchi, K., Tien, M.-H., and D'Souza, K., 2020. "Experimental forced response analysis of two-degree-of-freedom piecewise-linear systems with a gap". In International Design Engineering Technical Conferences and Computers and Information in Engineering Conference, Vol. 83969, American Society of Mechanical Engineers, p. V007T07A019.
- [13] Bagley, R. L., and Torvik, P., 1983. "A theoretical basis for the application of fractional calculus to viscoelasticity". *Journal of Rheology*, **27**(3), pp. 201–210.
- [14] Homaeinezhad, M., and Shahhosseini, A., 2020. "Fractional order actuation systems: theoretical foundation and application in feedback control of mechanical systems". *Applied Mathematical Modelling*, 87, pp. 625–

- 639.
- [15] Gaul, L., and Nitsche, R., 2001. "The Role of Friction in Mechanical Joints". *Applied Mechanics Reviews*, **54**(2), 03, pp. 93–106.
- [16] Sun, H., Ma, C., and Bernitsas, M. M., 2018. "Hydrokinetic power conversion using flow induced vibrations with nonlinear (adaptive piecewise-linear) springs". *Energy*, **143**, pp. 1085–1106.
- [17] Maistrenko, Y., and Kapitaniak, T., 1996. "Different types of chaos synchronization in two coupled piecewise linear maps". *Physical Review E*, **54**(4), p. 3285.
- [18] Tien, M.-H., and D'Souza, K., 2019. "Analyzing bilinear systems using a new hybrid symbolic-numeric computational method". *Journal of Vibration and Acoustics*, **141**(3).
- [19] Hsu, C.-L., and Tien, M.-H., 2023. "Parametric analysis of the nonlinear dynamics of a cracked cantilever beam". *Journal of Vibration and Acoustics*, **145**(3).
- [20] Ewins, D. J., 2000. *Modal testing: Theory and practice.* Baldock, England: Research Studies Press, UK.
- [21] Nakhla, M., and Vlach, J., 1976. "A piecewise harmonic balance technique for determination of periodic response of nonlinear systems". *IEEE Transactions on Circuits and Systems*, **23**(2), pp. 85–91.
- [22] Lau, S. L., and Zhang, W.-S., 1992. "Nonlinear Vibrations of Piecewise-Linear Systems by Incremental Harmonic Balance Method". *Journal of Applied Mechanics*, **59**(1), 03, pp. 153–160.
- [23] Xu, L., Lu, M., and Cao, Q., 2002. "Nonlinear vibrations of dynamical systems with a general form of piecewise-linear viscous damping by incremental harmonic balance method". *Physics Letters A*, **301**(1-2), pp. 65–73.
- [24] Saito, A., Castanier, M. P., Pierre, C., and Poudou, O., 2009. "Efficient nonlinear vibration analysis of the forced response of rotating cracked blades". *Journal of Computational and Nonlinear Dynamics*, **4**(1).
- [25] Tien, M.-H., and D'Souza, K., 2017. "A generalized bilinear amplitude and frequency approximation for piecewise-linear nonlinear systems with gaps or prestress". *Nonlinear Dynamics*, **88**(4), pp. 2403–2416.
- [26] Tien, M.-H., Hu, T., and D'Souza, K., 2018. "Generalized bilinear amplitude approximation and x-xr for modeling cyclically symmetric structures with cracks". *Journal of Vibration and Acoustics*, **140**(4).
- [27] Tien, M.-H., Hu, T., and D'Souza, K., 2019. "Statistical analysis of the nonlinear response of bladed disks with mistuning and cracks". *AIAA Journal*, **57**(11), pp. 4966–4977.
- [28] Altamirano, G. L., Tien, M.-H., and D'Souza, K., 2021. "A new method to find the forced response of nonlinear systems with dry friction". *Journal of Computational and Nonlinear Dynamics*.
- [29] Filippov, A., 1988. Differential Equations with Discontinuous Righthand Sides. Springer Netherlands, Netherlands.
- [30] Butcher, J., 1996. "A history of runge-kutta methods". *Applied Numerical Mathematics*, **20**(3), pp. 247–260.

- [31] Popp, K., and Stelter, P., 1990. "Stick-slip vibrations and chaos". *Philosophical Transactions: Physical Sciences and Engineering*, pp. 89–105.
- [32] Karnopp, D., 1985. "Computer simulation of stick-slip friction in mechanical dynamic systems". *Journal of Dynamic Systems, Measurement, and Control.*
- [33] Mora, P., and Place, D., 1994. "Simulation of the frictional stick-slip instability". *Pure and Applied Geophysics*, **143**(1), pp. 61–87.
- [34] Varsakelis, C., and Anagnostidis, P., 2016. "On the susceptibility of numerical methods to computational chaos and superstability". Communications in Nonlinear Science and Numerical Simulation, 33, pp. 118– 132.
- [35] Stefani, G., De Angelis, M., and Andreaus, U., 2021. "Numerical study on the response scenarios in a vibro-impact single-degree-of-freedom oscillator with two unilateral dissipative and deformable constraints". *Communications in Nonlinear Science and Numerical Simulation*, **99**, p. 105818.
- [36] Tien, M.-H., and D'Souza, K., 2019. "Transient dynamic analysis of cracked structures with multiple contact pairs using generalized HSNC". *Nonlinear Dynamics*, **96**(2), pp. 1115–1131.
- [37] Acary, V., and Brogliato, B., 2008. *Numerical methods for nonsmooth dynamical systems*. Springer-Verlag Berlin Heidelberg, Berlin.
- [38] Piiroinen, P. T., and Kuznetsov, Y. A., 2008. "An event-driven method to simulate filippov systems with accurate computing of sliding motions". *ACM Transactions on Mathematical Software (TOMS)*, **34**(3), pp. 1–24.
- [39] Bernardo, M., Budd, C., Champneys, A. R., and Kowalczyk, P., 2008. *Piecewise-smooth dynamical sys*tems: theory and applications, Vol. 163. Springer Science & Business Media.
- [40] Fu, Z.-F., and He, J., 2001. *Modal Analysis*. Elsevier Netherlands, Netherlands.
- [41] Zaslavskiî, G. M., Sagdeev, R. Z., Usikov, D. A., and Chernikov, A. A., 2009. *Weak Chaos and Quasi-Regular Patterns*. Cambridge University Press.
- [42] Mehrdad Pourkiaee, S., and Zucca, S., 2019. "A reduced order model for nonlinear dynamics of mistuned bladed disks with shroud friction contacts". *Journal of Engineering for Gas Turbines and Power,* **141**(1).
- [43] Krack, M., Panning-von Scheidt, L., Wallaschek, J., Siewert, C., and Hartung, A., 2013. "Reduced order modeling based on complex nonlinear modal analysis and its application to bladed disks with shroud contact". *Journal of Engineering for Gas Turbines and Power*, 135(10).
- [44] Zucca, S., Firrone, C. M., and Gola, M., 2013. "Modeling underplatform dampers for turbine blades: a refined approach in the frequency domain". *Journal of Vibration and Control*, **19**(7), pp. 1087–1102.
- [45] Laxalde, D., Thouverez, F., and Lombard, J.-P., 2010. "Forced response analysis of integrally bladed disks with friction ring dampers". *Journal of Vibration and Acoustics*, **132**(1).

- [46] D'Souza, K. X., and Epureanu, B. I., 2012. "A statistical characterization of the effects of mistuning in multistage bladed disks". *Journal of Engineering for Gas Turbines and Power*, **134**(1).
- [47] Kurstak, E., and D'Souza, K., 2020. "A statistical characterization of the effects and interactions of small and large mistuning on multistage bladed disks". *Journal of Engineering for Gas Turbines and Power,* **142**(4).
- [48] D'Souza, K., Jung, C., and Epureanu, B. I., 2013. "Analyzing mistuned multi-stage turbomachinery rotors with aerodynamic effects". *Journal of Fluids and Structures*, **42**, pp. 388–400.
- [49] Kurstak, E., and D'Souza, K., 2018. "Multistage blisk and large mistuning modeling using fourier constraint modes and prime". *Journal of Engineering for Gas Turbines and Power*, **140**(7).
- [50] Kurstak, E., Wilber, R., and D'Souza, K., 2019. "Parametric reduced order models for bladed disks with mistuning and varying operational speed". *Journal of Engineering for Gas Turbines and Power,* **141**(5).
- [51] Tien, M.-H., Hu, T., and D'Souza, K., 2019. "Efficient analysis of cyclic symmetric structures with mistuning and cracks". In AIAA Scitech 2019 Forum, p. 0489.
- [52] Balageas, D., Fritzen, C.-P., and Güemes, A., 2010. *Structural Health Monitoring*, Vol. 90. John Wiley & Sons.
- [53] Baek, S., and Epureanu, B., 2020. "Contact model identification for friction ring dampers in blisks with reduced order modeling". *International Journal of Non-Linear Mechanics*, **120**, p. 103374.
- [54] Friswell, M. I., and Penny, J. E., 2002. "Crack modeling for structural health monitoring". *Structural Health Monitoring*, **1**(2), pp. 139–148.